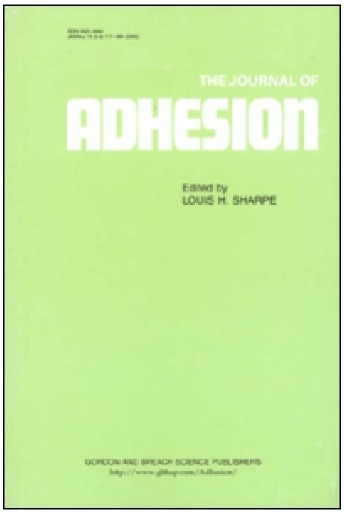

The Journal of Adhesion
Publication details, including instructions for authors and subscription information:
http://www.informaworld.com/smpp/title~content=t713453635

Role of Surface Polarity in the Evolution of Polymer Surface Properties in Liquid Medium

Jean Waku[a]; Alain Carre[a]
[a] Corning SAS, Corning European Technology Center, Avon, France

To cite this Article Waku, Jean and Carre, Alain(2010) 'Role of Surface Polarity in the Evolution of Polymer Surface Properties in Liquid Medium', The Journal of Adhesion, 86: 8, 874 — 889
To link to this Article: DOI: 10.1080/00218464.2010.498744
URL: http://dx.doi.org/10.1080/00218464.2010.498744

The Journal of Adhesion, 86:874–889, 2010
Copyright © Taylor & Francis Group, LLC
ISSN: 0021-8464 print/1545-5823 online
DOI: 10.1080/00218464.2010.498744

Taylor & Francis
Taylor & Francis Group

Role of Surface Polarity in the Evolution of Polymer Surface Properties in Liquid Medium

Jean Waku and Alain Carre
Corning SAS, Corning European Technology Center, Avon, France

Contact angle hysteresis of polystyrene and four modified polystyrenes, containing polar sulfonic acid and carboxylic acid groups, have been evaluated in a two-phase liquid system. Water contact angles have been measured in octane and octane contact angles have been measured in water. It has been demonstrated that wetting characteristics of polystyrene modified with sulfonic acid and carboxylic acid groups can be reversely triggered from polar in the presence of water to non-polar in the presence of octane. A contact angle hysteresis varying from 7 to 88° has been observed and a relationship between the contact angle hysteresis and the polymer surface polarity has been established. The fast kinetics of the wetting transition indicates that such polymers can permit external stimuli-induced modulation of their structures.

Keywords: Adaptive surface properties; Contact angle hysteresis; Mobile interfaces; Wetting transition

1. INTRODUCTION

Materials that change their structure and properties in response to external chemical and/or physical stimuli, such as temperature, pH, light, and electric fields, are continuing to gain considerable research attention [1]. These materials sense a stimulus as a signal (*sensor function*), judge the magnitude of this signal (*processor function*) and, as a consequence, alter their function in direct response (*effectors function*). They are called smart surfaces [2,3] or stimuli-responsive polymers [4,5], and have permitted external stimuli-induced modulation of their structures and on-off switching of their respective functions at molecular levels [6].

Received 11 September 2009; in final form 2 April 2010.

Address correspondence to Jean Waku, Corning SAS, Corning European Technology Center, 7 bis, Avenue de Valvins, 77210 Avon, France. E-mail: waku_jean@yahoo.fr

This change in the structure and the structure properties allows the control of interfacial free energy and surface wettability. This ability to control interfacial and surface attributes has been applied in applications such as adhesion of metal to polymers [7–9], modification of surface properties for chromatographic separators [10–13], and surfaces for regulated cell adhesion and detachment [14,15].

One way to characterize the change in structure of such material is to quantify the contact angle hysteresis by measuring contact angles. When subjected to the right stimuli, the surface of stimuli-responsive polymers reorganizes or structures itself so as to achieve the lowest possible interfacial tension. Therefore, measuring contact angles, before and after the reorganization helps define a contact angle hysteresis which is characteristic of the structure change.

In this paper, we report results of the study of contact angle hysteresis on polystyrene and four polystyrene substrates modified with acidic polar groups. It has been observed that polystyrene containing acidic polar groups can behave as stimuli-responsive polymers switching from hydrophilic in the presence of a polar liquid (water) to hydrophobic in the presence of a non-polar liquid (octane). While surface rearrangement has been reported as being a relatively slow process at room temperature for rigid solids [16,17], we have found that polystyrene modified with acidic polar groups can rearrange and achieve the lowest possible interfacial tension within minutes, even seconds. The hypothesis of a migration or a selective orientation of polar groups at the surface has been validated by studying the contact angle kinetics in water and octane. Moreover, a clear relationship has been established between the contact angle hysteresis and the presence of polar groups at the polymer surface.

2. THEORETICAL

2.1. Contact Angle Measurements

Contact angle measurements are widely used for quantifying surface energies of solids [18,19]. The drop of a liquid for which surface tension is known is deposited on the solid in the presence of a non-miscible fluid which can be air or another liquid. After deposition, the drop spreads until an equilibrium is attained providing the triple line liquid-solid-non-miscible fluid from which the contact angle, θ, can be measured (Fig. 1a).

If the solid is tilted at a given angle, contact angles on both sides of the drop might be different. In that case, advancing and receding angles can be observed (θ_a and θ_r). These can be defined as the limit

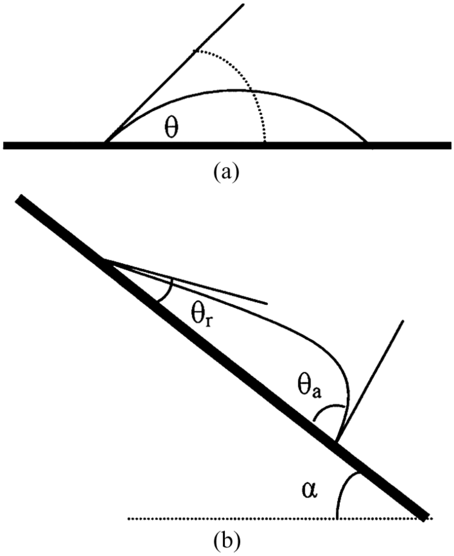

FIGURE 1 (a) Liquid drop on a solid (tilting angle = 0). (b) Liquid drop on a solid (tilting angle = α).

angles on both drop sides before the drop starts sliding on the inclined plane (Fig. 1b). Contact angle hysteresis can, therefore, be defined as the subtraction of the receding angle from the advancing angle:

$$H = \theta_a - \theta_r. \tag{1}$$

Another technique for observing a contact angle hysteresis is by adding and removing the liquid to the drop on the solid (tilting angle = 0). If liquid is added to the drop, the contact line defined by the triple point will advance until the drop reaches an equilibrium providing a new triple line. The maximum measured angle, just before the triple line advances, will be the advancing contact angle. Inversely, if the liquid is removed from the drop then the contact angle will recede until reaching a minimum value before the receding of the triple line. The minimum measured angle, just before the triple line recedes, will be the receding contact angle.

We have used a third technique for measuring the contact angle hysteresis on solid polymers which consists of a two-phase liquid system. Water contact angle has been measured on a solid immersed in octane and inversely octane contact angle has been measured on the same solid immersed in water (Figs. 2a and 2b). This system has the advantage of allowing finite contact angles to be obtained for solids

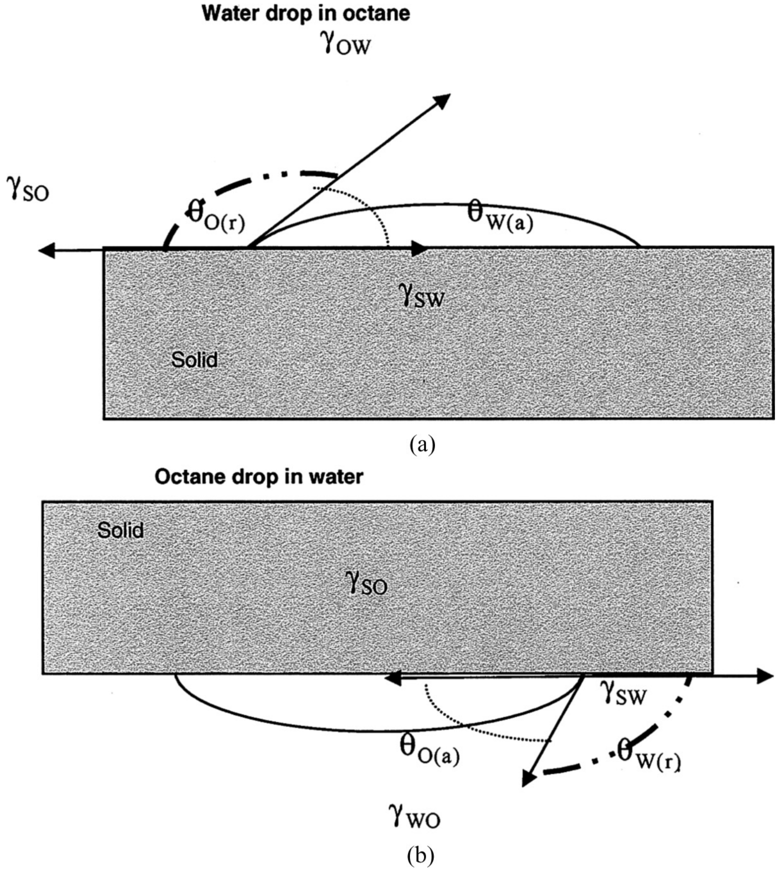

FIGURE 2 (a) Contact angle of water in octane. To gain contact with solid, the water drop displaces octane. The measured angle is the advancing water angle while the complementary angle is the octane receding angle and $\theta_{W(a)} + \theta_{O(r)} = 180°$. (b) Contact angle of octane in water. To gain contact with solid, the octane drop displaces water. The measured angle is the advancing octane angle while the complementary angle is the water receding angle and $\theta_{O(a)} + \theta_{W(r)} = 180°$. The drop is underneath the solid substrate in the case of octane drop in water because of the relative density of water and octane.

on which most normal liquids would spread spontaneously, and to eliminate contact angle variation due to evaporation. Another advantage provided by this technique is the finite assessment of contact angle hysteresis [20].

The contact angle hysteresis can be the result of surface attributes such as heterogeneity [21–26], roughness [27–30], and swelling [31–36]. However, polymer surface reorganization can also contribute to the contact angle hysteresis [20,37–43]. This is the main focus of this paper.

2.2. Determination of the Contact Angle Hysteresis

Contact angle measurements have been undertaken using the two-phase n-octane/water and water/n-octane liquid systems to assess the selective orientation of polar groups at the surface (Figs. 2a and 2b). As demonstrated by Shanahan *et al.* [44], when measuring the water contact angle in octane, water displaces octane to gain contact with the solid. Therefore, we measure the advancing water contact angle, $\theta_{W(a)}$, and the supplementary angle is the receding octane contact angle, $\theta_{O(r)}$:

$$\theta_{W(a)} + \theta_{O(r)} = 180^{\circ}. \tag{2}$$

Inversely, when measuring octane contact angle in water, octane displaces water to gain contact with the solid. Therefore, we measure the advancing octane contact angle, $\theta_{O(a)}$, and the supplementary angle is the water receding angle, $\theta_{W(r)}$:

$$\theta_{O(a)} + \theta_{W(r)} = 180^{\circ}. \tag{3}$$

Combining (1) and (3), the contact angle hysteresis can be expressed as:

$$\begin{aligned} \mathrm{H} &= \theta_{W(a)} - \theta_{W(r)}, \quad \text{or} \\ \mathrm{H} &= \theta_{W(a)} + \theta_{O(a)} - 180^{\circ}. \end{aligned} \tag{4}$$

2.3. Polar Component of the Solid Surface Free Energy

We consider the contact region between the solid, water, and n-octane. In the case that we measure the water contact angle in octane, Young's equation can be written:

$$\gamma_{SO} = \gamma_{SW} + \gamma_{OW} \cdot \cos\theta_{W(a)}. \tag{5}$$

As a first approximation, we will consider that solid-liquid interactions can be classified either as non-polar (dispersion forces) or polar. Polar interactions will include dipolar, acid-base, or ionic forces. Using the Dupré equation, the solid-liquid interfacial free energy is given by:

$$\gamma_{SW} = \gamma_S + \gamma_W - W_{SW}, \tag{6}$$

$$\gamma_{SO} = \gamma_S + \gamma_O - W_{SO}, \tag{7}$$

wherein γ refers to interfacial or surface tension, W refers to the work of adhesion, and subscripts O and W refer to n-octane and water.

The work of adhesion (W_{SW}) between the solid and water can be expressed as the sum of the dispersive and the polar components of the energy of solid-liquid interaction (I_{SW}):

$$W_{SW} = I^D_{SW} + I^P_{SW}, \tag{8}$$

wherein the superscripts D and P refer to dispersive and polar contributions.

Similarly, the work of adhesion between the solid and octane is defined as:

$$W_{SO} = I^D_{SO} + I^P_{SO}, \tag{9}$$

(However, as demonstrated below and as octane is purely non-polar, the term $I^P_{SO} = 0$).

The dispersive and the polar component of the work of adhesion can be expressed as a geometric mean of dispersive and polar component of surface tensions of the solid substrate, S, and the liquid, L, according to the model developed by Owens and Wendt [45]:

$$I^D_{SL} = 2\sqrt{\gamma^D_S \cdot \gamma^D_L} \tag{10}$$

$$I^P_{SL} = 2\sqrt{\gamma^P_S \cdot \gamma^P_L}, \tag{11}$$

where the superscripts D and P refer to dispersive and polar components of the surface free energies.

Combining (6)–(11) we obtain:

$$\gamma_{SW} = \gamma_S + \gamma_W - 2(\gamma^D_S \cdot \gamma^D_W)^{1/2} - 2(\gamma^P_S \cdot \gamma^P_W)^{1/2} \tag{12}$$

$$\gamma_{SO} = \gamma_S + \gamma_O - 2(\gamma^D_S \cdot \gamma^D_O)^{1/2} - 2(\gamma^P_S \cdot \gamma^P_O)^{1/2} \tag{13}$$

Octane is purely non-polar,

$$\gamma^P_O = 0 \tag{14}$$

and

$$\gamma^D_W \approx \gamma^D_O = 21.6 \; vs. \; 21.3\,\mathrm{mJ/m^2}. \tag{15}$$

Combining Equations (5) and (12)–(15) we obtain the polar component of the solid surface free energy when the solid is immersed in octane:

$$\gamma_S^P = \gamma_{S(O)}^P = \frac{[\gamma_W - \gamma_O + \gamma_{OW} \cdot \cos\theta_{W(a)}]^2}{4\gamma_W^P}. \tag{16}$$

In the inverse situation where we measure the contact angle of an octane drop in water, Young's equation can be written:

$$\gamma_{SW} = \gamma_{SO} + \gamma_{OW} \cdot \cos\theta_{O(a)}. \tag{17}$$

Combining Equations (12)–(15) and (17) we obtain the polar component of the solid surface free energy when the solid is immersed in water:

$$\gamma_S^P = \gamma_{S(W)}^P = \frac{[\gamma_W - \gamma_O - \gamma_{OW} \cdot \cos\theta_{O(a)}]^2}{4\gamma_W^P}. \tag{18}$$

2.4. Energy of Polar Interactions

In the case of a water drop on a solid in n-octane, the relationships of Young and Fowkes Equations can be combined to obtain the energy of polar interactions per unit of area [20]:

$$I_{SW(O)}^P \approx \gamma_W - \gamma_O + \gamma_{OW} \cdot \cos\theta_{W(a)}. \tag{19}$$

$I_{SW(O)}^P$ represents the polar interaction between the solid and water, in the presence of octane.

In the case of the inverse situation where we measure the contact angle of n-octane on a solid in water we obtain:

$$I_{SW(W)}^P \approx \gamma_W - \gamma_O - \gamma_{OW} \cdot \cos\theta_{O(a)}. \tag{20}$$

$I_{SW(W)}^P$ is the energy of polar interactions between the solid and water, when the polymer is immersed in water.

Ideally, $I_{SW(O)}^P$ and $I_{SW(W)}^P$ should be equal. Subtracting (20) to (19) would give:

$$\cos\theta_{W(a)} + \cos\theta_{O(a)} = 0 \Longleftrightarrow \theta_{W(a)} + \theta_{O(a)} = 180^\circ \tag{21}$$

As defined in paragraph 2.2., the contact angle hysteresis (H) in the two-phase n-octane/water and water/n-octane liquid systems can be expressed as:

$$H = \theta_{W(a)} + \theta_{O(a)} - 180^\circ. \qquad (22) = (4)$$

3. MATERIALS

Polystyrene (PS) and four modified polystyrene substrates containing polar acidic groups have been studied: sulfonated polystyrene (SPS), polystyrene copolymerized with maleic anhydride (PSAM), plasma-treated Corning® polystyrene for cell culture [polystyrene treated for cell culture (PSTCT)], and Corning CellBIND® surface (CellBIND). Those polymers possess a hydrophobic backbone made of methylene groups that bear hydrophilic acidic groups.

Corning polystyrene cell culture treated vessels (PSTCT) are surface modified using either corona discharge (flasks, dishes, and microplates) or gas-plasma (roller bottles and culture tubes). These processes generate highly energetic oxygen ions and free radicals which graft onto the surface polystyrene chains so that the surface becomes hydrophilic and negatively charged. The more the oxygen is incorporated onto the surface the more hydrophilic it becomes.

The Corning CellBIND Surface is prepared with a technology that uses microwave plasma. The process incorporates significantly more oxygen into the cell culture surface, rendering it more hydrophilic. X-ray photoelectron spectroscopy (XPS) shows that the amount of oxygen incorporated into the Corning CellBIND Surface is more than 60% higher than with the traditional tissue culture surface treatment with 29 *versus* 17.2% of oxygen atoms (http://www.corning.com/lifesciences/us_canada/en/technical_resources/surfaces/culture/corning_cellbind_polystyrene.aspx).

PS, PSTCT, and CellBIND cell culture dishes where directly purchased from Corning Life Sciences (Corning Inc., Corning, NY, USA) (http://catalog2.corning.com/Lifesciences/en-US/Shopping/index.aspx).

Pellets of PSAM, polystyrene copolymerized with maleic anhydride, copolymerization rate of 7 mol% and 14 mol%, were purchased from Sigma-Aldrich (http://www.sigmaaldrich.com). Those pellets were compounded, extruded, and molded into 32-mm discs using the DSM micro-extruder machine (http://www.xplore-together.com/products.htm) with the equipment settings in Table 1.

TABLE 1 Molding and Extrusion Settings for Producing 32 mm PSAM Discs with DSM Mico-Extruder Machine

Pellets weight (g)	16
Screw's speed (rpm)	100
Screw's acceleration (rpm/s)	100
Extrusion temperature (°C)	190
Molding temperature (°C)	220

After molding, the maleic anhydride groups were hydrolyzed by immersing PSAM discs for 3 hours in a basic solution (pH = 9), followed by rinsing with deionised water and drying at room temperature with a nitrogen gun.

Polystyrene with sulfonation rate ranging from 3 to 22 mol% were synthesized by homogeneous sulfonation [46–48]. Extrusion and compounding of sulfonated polystyrene into discs was not possible due to the cross-linking of the material favored by elevated extrusion temperature. As a consequence, the polymer turned dark. Cross-linking was confirmed by the polymer insolubility in dichloromethane [47,48]. Thus, sulfonated polystyrene was dissolved in a mixture of equal volumes of toluene and acetone (2 to 5 wt% of sulfonated polystyrene in the mixture), spin-coated on polystyrene discs at 1500 rpm for 30 seconds, and dried at 80°C for 1 hour.

4. RESULTS

4.1. Contact Angle Data and Mechanism of Wettability Change

Samples were first measured in octane (water drop in octane) and then in water (octane drop in water). After the measurement of the advancing water contact angle in octane ($\theta_{W(a)}$), the sample was dried at room temperature with a nitrogen gun and immediately immersed in water (Figs. 2a and 2b) for the measurement of the advancing octane contact angle in water ($\theta_{O(a)}$). The aim was to assess the change in surface wetting and surface free energy.

As demonstrated with Eq. (21), one would expect to see the sum of $\theta_{W(a)}$ and $\theta_{O(a)}$ to be 180° in the absence of contact angle hysteresis, which is not the case. The summary of contact angle in Table 2 clearly indicates that hysteresis is observed on all tested polymers.

TABLE 2 Water Contact Angle in n-octane ($\theta_{W(a)}$), n-octane Contact Angle in Water ($\theta_{O(a)}$), and Contact Angle Hysteresis (H)

Polymer	$\theta_{W(a)}$ (°)	$\theta_{O(a)}$ (°)	$\theta_{W(a)} + \theta_{O(a)}$ (°)	H (°)	ΔH (°)*
PS	170	73	243	63	0
PSTCT	170	80	250	70	7
PSS 8.5 mol%	170	115	285	105	42
PSAM 14 mol%	174	132	305	125	62
CellBIND	156	175	331	151	88

ΔH (°)* is the contribution of surface chemical functions to contact angle hysteresis, polystyrene being considered as a reference. Standard deviation on contact angles ≤1°.

We used Eq. (16) to compute the polar component of the surface free energy when the sample is immersed in octane ($\gamma^{P}_{S(O)}$) and Eq. (18) for the polar component of the surface free energy when the sample is immersed in water ($\gamma^{P}_{S(W)}$). One would also expect γ^{P}_{S} in octane and γ^{P}_{S} in water to be equal, which is not the case. Let us examine in detail the changes on the surface of PSS 8.5 mol% sample. When immersed in octane, the surface turns from polar to non-polar and γ^{P}_{S} decreases from 8.8 down to 0 mJ/m^2 in 10 minutes (Fig. 3). When immersed in water, γ^{P}_{S} increases from 0 up to 28 mJ/m^2 in 1 minute, reaching a value higher than the initial value before immersion in octane (Fig. 4). This trend was also observed on other polystyrenes modified with polar acidic groups (Tables 3–5). We believe that the observed variation of the polar properties of the polystyrene substrate result from a reorganization or migration of polar groups at the surface according to the nature of the environmental medium (polar or non-polar). These data confirm that the polymer polarity cannot be considered as an intrinsic property of the material but rather as a property that can be induced [49] by the medium in contact with the polymer surface. The fact that this change occurs within minutes indicates fast kinetics. Therefore, these polystyrene modified with polar acidic groups can be used as smart surfaces or stimuli-responsive polymers, the properties of which can be switched from hydrophilic to hydrophobic by a change in the medium (Figs. 5a and 5b). The switch from hydrophilic to hydrophobic, then from hydrophobic to hydrophilic, has been checked several times.

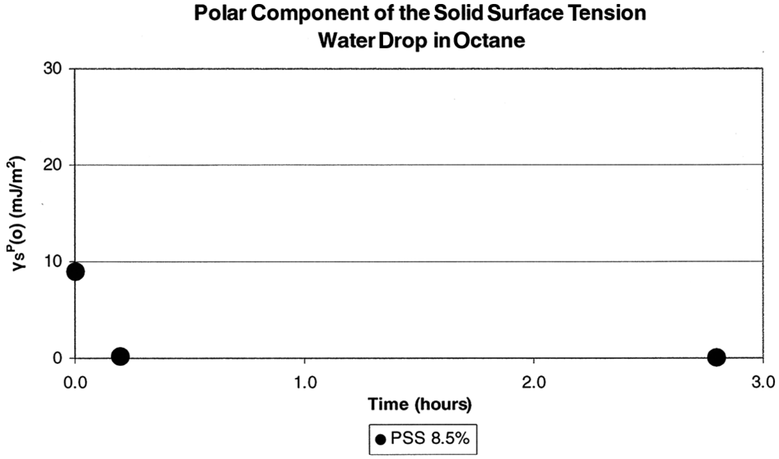

FIGURE 3 Variation of the polar component of the solid surface free energy. Water contact angle is measured in octane.

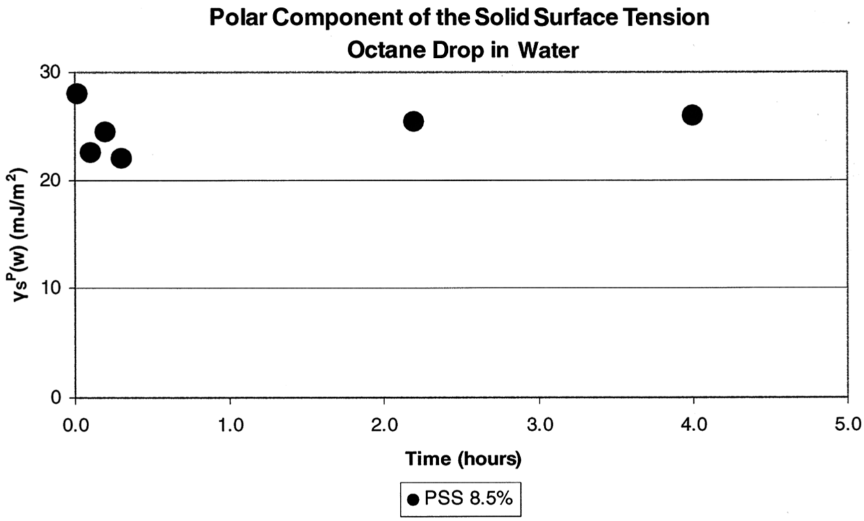

FIGURE 4 Variation of the polar component of the solid surface free energy. Octane drop contact angle is measured in water.

TABLE 3 Variation of γ_S^P in Octane. Water Contact Angle is Measured on Polymer Immersed in Octane

Polymer	Immersion time in octane (hours)	0.003	0.2	2.8
PS	$\gamma_{S(O)}^P$ (mJ/m^2)	0.5	0.1	0.0
PSTCT	$\gamma_{S(O)}^P$ (mJ/m^2)	18.7	2.9	0.0
PSS 8.5 mol%	$\gamma_{S(O)}^P$ (mJ/m^2)	8.8	0.2	0.0
PSMA 14 mol%	$\gamma_{S(O)}^P$ (mJ/m^2)	0.0	0.0	0.0
CellBIND	$\gamma_{S(O)}^P$ (mJ/m^2)	4.1	4.0	0.1

TABLE 4 Variation of γ_S^P in Water. Octane Contact Angle is Measured on Polymer Immersed in Water

Polymer	Immersion time in water (hours)	0.02	0.1	0.2	0.3	2.2	4.0
PS	$\gamma_{S(W)}^P$ (mJ/m^2)	5.2	6.3	7.4	7.7	5.6	6.3
PSTCT	$\gamma_{S(W)}^P$ (mJ/m^2)	3.7	6.8	7.1	7.9	8.8	8.8
PSS 8.5 mol%	$\gamma_{S(W)}^P$ (mJ/m^2)	28.0	22.5	24.5	22.0	25.4	25.9
PSMA 14 mol%	$\gamma_{S(W)}^P$ (mJ/m^2)	9.3	30.0	30.0	32.6	36.0	35.4
CellBIND	$\gamma_{S(W)}^P$ (mJ/m^2)	50.2	50.4	51.0	51.0	51.0	51.0

TABLE 5 Polar Energy Transition. γ_S^P in Octane (Water Drop in Octane) is Subtracted from γ_S^P in Water (Octane Drop in Water)

Polymer	$\Delta\gamma_S^P$ (mJ/m^2)	$\Delta\gamma_S^P$ (mJ/m^2)*
PS	6.3	0
PSTCT	8.8	2.5
PSS 8.5 mol%	25.9	19.6
PSMA 14 mol%	35.4	29.1
CellBIND	50.9	44.6

$\Delta\gamma_S^P$ (mJ/m^2)* is the contribution of surface chemical functions taking polystyrene as a reference. Polar energy transition has been determined using contact angle measurements at equilibrium (after 3 and 5hours of immersion).

If we assume that the polar component of surface free energy is proportional to the density of polar groups on the surface, then the migration of polar groups to and from the surface has to be considered as part of the effects that contribute to the change of polar free energy. Furthermore, subtracting $\gamma_{S(O)}^P$ when the polymer is immersed in octane from $\gamma_{S(W)}^P$ when the polymer is immersed in water, we found an energy transition of 19.6 mJ/m^2, which, to our knowledge, is reported for the first time. Mendez *et al.* [4] reported contact angle transitions on stimuli-responsive polymers containing carboxylic acid groups. A relationship between the transition range and the amount of carboxylic groups was even established. The difference between the work of the Mendez group and the present paper is that their stimuli-responsive polymers comprised poly(N-isopropylacrylamide),

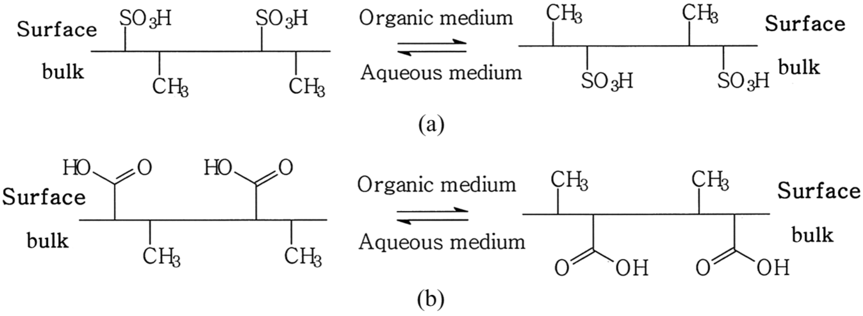

FIGURE 5 (a) Selective migration of SO_3H at the surface of sulfonated polystyrene (SPS). (b) Selective migration of CO_2H at the surface of plasma oxygen-treated polystyrene (PSTCT and CellBIND) and polystyrene copolymerized with maleic anhydride (PSAM).

TABLE 6 Water Contact Angle in n-octane ($\theta_{W(a)}$), n-octane Contact Angle in Water ($\theta_{O(a)}$), and Energy of Polar Interactions (I^{o} and I^{w})

Polymer	$\theta_{W(a)}$ (°)	$\theta_{O(a)}$ (°)	H (°)	$I^{P}_{SW(W)}$ (mJ/m^2)	$I^{P}_{SW(O)}$ (mJ/m^2)
PS	170	73	63	36	1
PSTCT	170	80	70	42	1
PSS 8.5 mol%	170	115	105	73	1
PSAM 14 mol%	174	132	125	85	0.5
CellBIND	156	175	151	102	4.8

Standard deviation on contact angles <1°.

a thermoresponsive polymer, that was synthesized on self-assembled monolayers that contained carboxylic acid groups. While the carboxylic acid groups played a clear role in the transition range, the wetting transition was still the consequence of a structure change of poly(N-isopropylacrylamide) under the effect of temperature.

To study the consequence of surface polarity on the hysteresis, polar interactions $I^{P}_{SW(W)}$ and $I^{P}_{SW(O)}$ were calculated (Table 6) by using Eqs. (20) and (19). There is an indication in Table 6 that contact angle hysteresis evolves with the polymer polarity ($I^{P}_{SW(W)}$ and $I^{P}_{SW(O)}$). This evolution is even clearer when the contact angle hysteresis is plotted as a function of polar interactions when the polymer surface is immersed in water ($I^{P}_{SW(W)}$). The linear relationship clearly indicates that the contact angle hysteresis is directly proportional to the polar

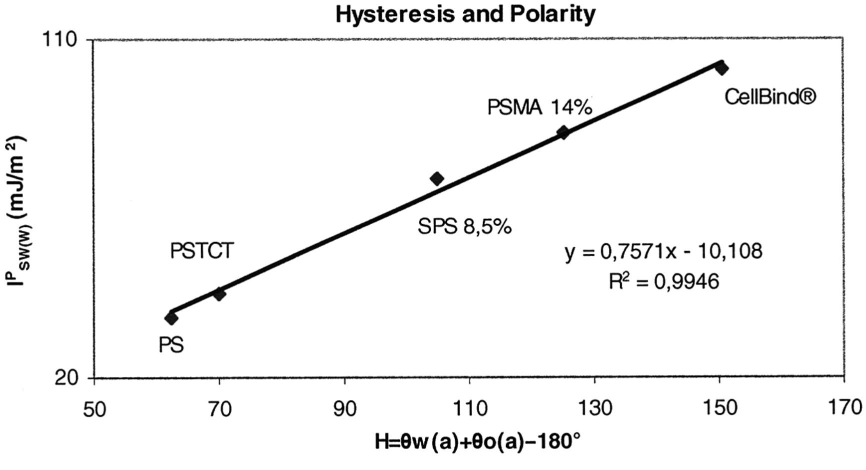

FIGURE 6 Relationship between polymer polarity and contact angle hysteresis.

interactions $I^{P}_{SW(W)}$ (Fig. 6) as observed by Shanahan *et al.* with a series of eight polymers of very different polarity [50].

5. DISCUSSION

As described in the introduction, the contact angle hysteresis can be the result of surface attributes such as roughness. The surface roughness of polystyrene (PS), polystyrene treated cell culture (PSTCT), and CellBIND has been checked and we have found similar roughness on all tested samples with arithmetic roughness (R_a) ranging from 2 to 8 nm (Table 7). Thus, a variable roughness cannot explain the contact angle hysteresis measured on each substrate.

One might also argue that polymer swelling in a liquid can induce contact angle hysteresis. One has to keep in mind that the wetting hysteresis reported in this work, in either water or octane, is very fast and reversible (Figs. 3 and 4). Moreover, references linking contact angle hysteresis to swelling, liquid retention, or surface imperfection (21–36), report moderate contact angle hysteresis below or equal to 35° and none of the polymers cited demonstrate both hydrophobic and hydrophilic properties. As the main result of our work, polystyrene surfaces modified with sulfonic or carboxylic acid groups display large contact angle hysteresis, likely resulting from the migration or orientation of these groups as a function of the nature of the contacting medium. However, we acknowledge that in addition to the polymer chain orientation mechanism discussed above, other effects, including liquid penetration and surface swelling, can also have contributed to some extent to the observed contact angle hysteresis.

As a practical application, polystyrene substrates described in this study were used in cell culture. The hydrophobic-hydrophilic switching ability of surfaces was successfully used to facilitate cell harvesting by changing the liquid medium. Only substrates modified with sulfonic or carboxylic acidic functions showed this possibility.

TABLE 7 Surface Roughness of Polymers

Polymer	Ra (nm)	Std. dev. (nm)
PS	2.2	0.1
PSTCT	1.8	0.1
PSS 8.5 mol%	8	2
PSMA 14 mol%	2.9	0.2
CellBIND	2.1	0.2

6. CONCLUSION

The contact angle hysteresis of four polystyrenes modified with hydrophilic acidic compounds has been evaluated in a two-phase liquid system. Water contact angles have been measured in octane and octane contact angles have been measured in water. A contact angle hysteresis varying from 7 to 88° has been observed and a relationship between the contact angle hysteresis and the polymer surface polarity has been established. While effects such as liquid penetration and surface swelling can contribute to the contact angle hysteresis, the fast kinetics and the reversibility of contact angle variation suggest in this work that polymer chain orientation is the main contributor to the phenomena. The fast kinetics of the contact angle hysteresis has permitted the external stimuli-induced modulation of structures of the studied polymers.

REFERENCES

[1] Luzinov, I., Minko, S., and Tsukruk, V. V., *Prog. Polym. Sci.* **29**, 635–698 (2004).

[2] Liao, K.-S., Fu, H., Wan, A., Batteas, J. D., and Bergbreiter, D. E., *Langmuir* **25** (1), 26–28 (2003).

[3] Zhou, F. and Huck, W. T. S., *Phys. Chem. Chem. Phys.* **8**, 3815–3823 (2006).

[4] Mendez, S., Linnea, K. L., and Lopez, P. G., *Langmuir* **19**, 8115–8116 (2003).

[5] Okano, T., *Biorelated Polymers and Gels*, (Academic Press, San Diego, 1999), p. 1.

[6] Okano, T., Bae, Y. H., Jacobs, H., and Kim, S. W., *J. Controlled Release* **11**, 255–265 (1990).

[7] Lavielle, L., Nakajima, K., and Schultz, J., *J. Applied Polymer Science* **46**, 1045–1050 (1992).

[8] Schultz, J., Carré, A., and Mazeau, C., *J. Adhesion and Adhesives* **4**, 163–168 (1984).

[9] Schultz, J., Lavielle, L., Carré, A., and Comien, P., *J. Material Science* **24**, 4363–4369 (1989).

[10] Kanazawa, H., Yamamoto, K., Matsushima, Y., Takai, N., Kikuchi, A., Sakurai, Y., and Okano, T., *Anal. Chem.* **68**, 100–105 (1996).

[11] Kanazawa, H., Yamamoto, K., Matsushima, Y., Takai, N., Kikuchi, A., Sakurai, Y., and Okano, T., *Anal. Chem.* **69**, 823–830 (1997).

[12] Kanazawa, H., Sunamoto, T., Matsushima, Y., Kikuchi, A., and Okano, T., *Anal. Chem.* **72**, 5961–5966 (2000).

[13] Akiyama, Y., Kikuchi, A., Yamato, M., and Okano, T., *Langmuir* **20** (13), 5506–5511 (2004).

[14] Okano, T., Yamada, N., Sakai, H., and Sakurai, Y., *J. Biomed. Mater. Res.* **27**, 1243–1251 (1993).

[15] Okano, T., Yamada, N., Okuhara, M., Sakai, H., and Sakurai, Y., *Biomaterials* **16** (4), 297–303 (1995).

[16] Andrade, J. D., King, R. N., Ma, S. M., and Gregonis, D. E., *Journal of Colloids and Interface Science* **72** (3), 488–493 (1979).

[17] Anastasiadis, S. H., Retsos, H., Pispas, S., Hadjichristidis, N., and Neophytides, S., *Macromolecules* **36**, 1994–1999 (2003).

[18] Guiseppi-Elie, A., Wnek, G. E., and Wesson, S., *Langmuir* **2**, 508–513 (1986).

[19] Kloubek, J., *Langmuir* **5** (4), 1127–1130 (1989).

[20] Carre, A., Moll, S., Schultz, J., and Shanahan, M. E. R., *Adhesion* **11** (Elsevier Applied Science, London and New York, 1987), Ch. 6, pp. 82–95.

[21] Ruch, R. J. and Bartell, L. S., *Journal of Physical Chemistry* **64** (5), 513–519 (1960).

[22] Johnson, R. E., Jr. and Dettre, R. H., *Journal of Physical Chemistry* **69** (7), 1744–1750 (1964).

[23] Schwartz, L. W. and Garoff, S., *Langmuir* **1** (2), 219–230 (1985).

[24] Decker, E. L. and Garoff, S., *Langmuir* **12** (8), 2100–2110 (1996).

[25] Di Mundo, R., Palumbo, F., and D'Agostino, R., *Langmuir* **24** (9), 5044–5051 (2008).

[26] Zhang, J. and Han, Y., *Langmuir* **24** (3), 769–801 (2008).

[27] Bartell, F. E. and Shepard, J. W., *Journal of Physical Chemistry* **57** (4), 455–458 (1953).

[28] Kietzig, A.-M., Hatzikiriakos, S. G., and Englezos, P., *Langmuir* **25** (8), 4821–4827 (2009).

[29] Cortese, B., D'Amone, S., Manca, M., Viola, I., Cingolani, R., and Gigli, G., *Langmuir* **24** (6), 2712–2718 (2008).

[30] Jurak, M. and Chibowski, E., *Langmuir* **23** (20), 10156–10163 (2007).

[31] Hennig, A., Eichhorn, K.-J., Staudinger, U., Sahre, K., Rogalli, M., Stamm, M., Neumann, A. W., and Grundke, K., *Langmuir* **20**, 6685–6691 (2004).

[32] Tavana, H., Simon, F., Grunbke, K., Kwok, D. Y., Hair, M. L., and Neumann, A. W., *J. Colloid and Interface Sci.* **291**, 497–506 (2005).

[33] Lam, C. N. C., Kim, N., Hui, D., Hair, D. Y., Hair, M. L., and Neumann, A. W., *Colloids Surf. A Physicochem. Eng. Asp.* **189**, 265–278 (2001).

[34] Lam, C. N. C., Wu, R., Li, D., Hair, M. L., and Neumann, A. W., *Adv. Colloid Interface Sci.* **96**, 169–191 (2002).

[35] Tavana, H., Petong, N., Hennig, A., and Neumann, A. W., *J. Adhes.* **81**, 29–39 (2005).

[36] Yang, J., Han, J., Isaacson, K., and Kwok, D. Y., *Langmuir* **19**, 9231–9238 (2003).

[37] Muller, P., Sudre, G., and Théodoly, O., *Langmuir* **24** (17), 9541–9550 (2008).

[38] Fadeev, A. Y. and McCarthy, T. J., *Langmuir* **15** (11), 3759–3766 (1999).

[39] Yasuda, T., Miyama, M., and Yasuda, H., *Langmuir* **10**, 583–585 (1994).

[40] Holmes-Farley, S. R., Reamey, R. H., Nuzzo, R., McCarthy, T. J., and Whiteside, G., *Langmuir* **3**, 799–815 (1987).

[41] Kwok, D. Y. and Neumann, A. W., *Adv. Colloid Interface Sci.* **81**, 167–249 (1999).

[42] Koberstein, J. T., *Journal of Polymer Science, Part B: Polymer Physics* **42** (16), 2942–2956 (2004).

[43] Pan, F., Wang, P., Lee, K., Wu, A., Turro, N. J., and Koberstein, J. T., *Langmuir* **21** (8), 3605–3612 (2005).

[44] Shanahan, M. E. R., Cazeneuve, C., Carre, A., and Schultz, J., *Journal de Chimie Physique et de Physico-Chimie Biologique* **79** (3), 241–245 (1982).

[45] Owens, D. K. and Wendt, R. C., *J. Appl. Polym. Sci.* **13**, 1741–1747 (1969).

[46] Thaler, W., *Macromolecules* **16** (4), 623–628 (1983).

[47] Kučera, F. and Jančář, J., *Polymer Engineering and Science* **38** (5), 782–792 (1998).

[48] Martins, C. R., Ruggeri, G., and De Paoli, M.-A., *Journal of the Brazilian Chemical Society* **14** (5), 797–802 (2003).

[49] Carre, A., *J. Adhesion Sci. Technol.* **21** (10), 921–981 (2007).

[50] Shanahan, M. E. R., Carre, A., Moll, S., and Schultz, J., *Journal de Chimie Physique et de Physico-Chimie Biologique* **83** (5), 351–354 (1986).